



Cite this: *Soft Matter*, 2015,
11, 4818

Supramolecular self-assembly of linear oligosilsesquioxanes on mica – AFM surface imaging and hydrophilicity studies†

Anna Kowalewska,* Maria Nowacka, Adam Tracz and Tomasz Makowski

Linear oligomeric [2-(carboxymethylthio)ethylsilsesquioxanes] (LPSQ-COOH) adsorb spontaneously on muscovite mica and form smooth, well-ordered lamellar structures at the liquid–solid interface. Side carboxylic groups, having donor–acceptor character with regard to hydrogen bonds, are engaged both in multipoint molecule-to-substrate interactions and intermolecular cross-linking. The unique arrangement of silsesquioxane macromolecules, with COOH groups situated at the interface with air, produces highly hydrophilic surfaces of good thermal and solvolytic stability. Supramolecular assemblies of LPSQ-COOH were studied using atomic force microscopy (AFM), angle-resolved X-ray photoelectron spectroscopy (ARXPS) and attenuated total reflectance (ATR) FTIR spectroscopy. Comparative height profile analysis combined with ATR-FTIR studies of the spectral regions characteristic of carboxylic groups and C1s core level envelope by XPS confirmed specific interactions between LPSQ-COOH and mica.

Received 2nd April 2015,

Accepted 1st May 2015

DOI: 10.1039/c5sm00787a

www.rsc.org/softmatter

Introduction

Surface properties (wettability, chemical functionalities, and surface charge density) are extremely important for materials' applications of biomedical and biotechnological importance.^{1–4} One example is the modulation of adsorption of biomolecules to evoke diverse cellular responses. Biospecific materials should resemble a natural extracellular matrix (ECM), with which cell adhesion molecules interact. Typical chemical groups involved in immobilizing ligands for cell-surface studies are hydroxyls, amines and carboxylic acids that belong to the RGD sequence. Materials bearing carboxylic moieties are of particular interest because COOH groups provide an appropriate wettability for the adhesion of specific cell types.^{3,5} It has also been observed that some type of cells can interact more strongly with secreted fibronectin when adsorbed on surfaces bearing COOH groups.^{6–13} As a consequence, chondrogenic differentiation of human mesenchymal stem cells was observed.^{12,13}

Surface properties can be enhanced by an appropriate modification and structuring.^{14,15} Self-assembled materials mimicking an ECM have emerged as promising bioengineering tools as they can provide precisely tailored, chemically well-defined substrates.

Self-assembled monolayers (SAMs) made of amphiphilic molecules^{16,17} can be used for the preparation of bioactive substrates via surface-specific adsorption or covalent immobilization.² Analogously, physicochemical adsorption of surface-active polymers at the solid/liquid interface can produce polymeric self-assembled monolayers (PSAMs) that offer a variety of unique functionalities as well as improved surface stability and processability.^{18–21} PSAMs differ from typical SAMs because of conformational characteristics of macromolecular chains that depend on the type and density of grafting as well as polymer–substrate affinity. PSAMs can be prepared by grafting side- and end-functionalized copolymers onto a surface through “grafting-to” or surface-initiated polymerization methods.^{20,21} Both techniques have some disadvantages (steric factors can influence both grafting density and monomer diffusion to active polymerization sites). The thickness of end-grafted PSAMs can vary not only with the type and density of grafting but also with the energy of polymer–substrate interactions. Polymers consisting of surface-reactive repeating units tend to adsorb with chain axes extended parallel to the surface.¹⁸ The thickness of such planar PSAMs is close to the diameter of polymer chain but can depend on the flexibility of the polymer backbone.

The structures of SAMs and PSAMs strongly depend on the chemical properties of the solid surface, its morphology, adsorption mechanism and the nature of the forces operating at the boundary.^{22,23} For example, muscovite mica, which is a layered aluminosilicate $[KAl_2(Si_3AlO_{10})(OH)_2]$, can provide specific assistance in the surface-assembly of biomacromolecules.^{24–26} Muscovite is very susceptible to cleavage along the plane located in the

Centre of Molecular and Macromolecular Studies, Polish Academy of Sciences, Sienkiewicza 112, 90-363 Łódź, Poland. E-mail: anko@cbmm.lodz.pl;

Fax: +48 426803 261; Tel: +48 426803 235

† Electronic supplementary information (ESI) available: All synthetic details and structural characterization (NMR) as well as additional data concerning surface characterization and behavior of LPSQ-COOH in solution (DLS studies). See DOI: 10.1039/c5sm00787a

potassium layer. Exfoliation along that plane exposes large areas of molecularly smooth surface covered with potassium ions. The operating surface-induced mechanisms of adsorption on mica include cooperative, K^+ ion-mediated, surface–adsorbate interactions (adsorption, surface diffusion and 2-D growth).²⁴ The formation of surface salts between COOH groups and K^+ ions was proposed to be involved in the adsorption of *n*-alkanoic carboxylic acids^{27–30} and oligothiophene derivatives of butyric acid.³¹ Chemical modification of mica using reactive silanes was also reported.^{32–35} However, the process is difficult to control and sensitive to the applied reaction conditions.^{36–40}

We have found that muscovite mica can be easily modified using new linear oligosilsesquioxanes (LPSQ-COOH) functionalized with side 2-(carboxymethylthio)ethyl groups along their double-strand backbone. LPSQ-COOH can form spontaneously well-ordered and stable PSAM-type 2D nanolayers at the liquid–solid interface. The oligomers are immobilized unilaterally, with their siloxane backbone parallel to the surface, due to both multipoint substrate–adsorbate and adsorbate–adsorbate interactions. As a consequence, carboxylic groups attached at one side of the polymer chain are directed uniquely to the interface with air (Scheme 1). This makes the surface exceptionally hydrophilic and potentially chemoreactive. To the best of our knowledge, such structures have not been observed for any PSAMs before.

The proposed, very simple method of modification of muscovite mica offers better stability of the adsorbed layer compared to those prepared with small molecules. The arrangement of side carboxylic groups in LPSQ-COOH about the main backbone allows for its very efficient anchoring on the surface. The structure of LPSQ-COOH makes possible the formation of layered morphologies and accessibility of carboxylic groups, which cannot be obtained with mono-acids.

It is also possible to control the structure of the coating by adjusting the parameters of the coating process (concentration of the solution, composition of solvents, method and time of coating). The specific properties of self-assembled structures of LPSQ-COOH make the studied system very attractive for surface modification (including micropatterning) and bioengineering.

Experimental

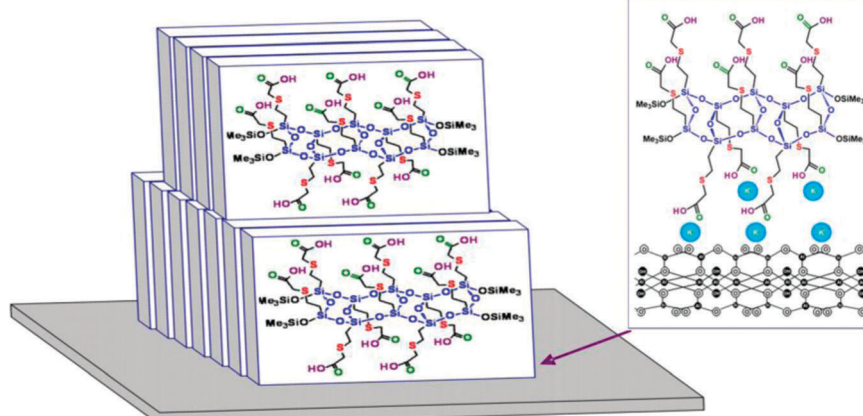
1. General information

Materials. Precursor oligo(vinylsilsesquioxanes) (LPSQ-Vi) (SEC in CH_2Cl_2 (RI): $M_n = 1000$, $M_w = 1200$, PDI = 1.2, (MALLS): $M_n = 2000$, $M_w = 3200$, PDI = 1.6.) were obtained with 67.5% yield by *in situ* polycondensation of cyclic tetravinylsiloxanetetraol.⁴¹ MALDI-TOF mass spectrometry was used as a method for the determination of the structure of LPSQ-Vi. Linear oligomers with chain ends terminated with trimethylsilyl groups were obtained. The results are consistent with those already reported by us.⁴¹ LPSQ-Vi were used as substrates for the synthesis of oligo[2-(carboxymethylthio)ethylsilsesquioxanes] (LPSQ-COOH) via UV-initiated thiol–ene addition of thioglycolic acid (all synthetic details and structural characterization (NMR) as well as simulated structures and additional data concerning surface characterization and behavior of LPSQ-COOH in solution [dynamic light scattering studies (DLS)] can be found in the ESI†). The structure of LPSQ-COOH oligomers self-assembled on mica was constructed using the HyperChem platform and modelled *in vacuo* using a molecular mechanics force field MM⁺ method (Polak–Ribiére/conjugate gradient optimization algorithm) and a semi-empirical PM3 method (single point energy calculations).

Muscovite mica tiles (V-1 grade, SPI Supplies/Structure Probe, Inc.) were freshly cleaved before use by removing the top layer with an adhesive tape.

2. Experimental procedures

Preparation of thin films of oligomeric linear silsesquioxanes on solid supports. Polymers (LPSQ-COOH or LPSQ-Vi) were dissolved in dry solvent [pure THF or a mixture of toluene and dioxane (v/v = 1 : 2)] at a given concentration. The solutions were filtered through a 0.2 μ m PTFE filter and placed in a vessel. Dip coating was carried out at room temperature by the immersion of a freshly cleaved muscovite mica support in the polymer solution for a given time (t_i). Supports were mounted and moved vertically with a motorized linear slide (Zaber Technologies Inc.) (rate of immersion/extraction = 4 mm s⁻¹). The volume of liquid and the immersion level were constant. Dip-coated supports



Scheme 1 Arrangement of oligo[2-(carboxymethylthio)-ethylsilsesquioxane] chains adsorbed on the surface of muscovite mica.

were then placed in a closed container and left for drying at room temperature for one day. Their surface was analyzed with AFM (tapping mode). In the spin coating technique, the dissolved polymer was spun onto cleaned mica supports horizontally attached on a rotating chuck (Bidtec SP100, spinning rate 700 rpm). The experiments were carried out in air at room temperature (24 °C).

Washing tests were made using mica supports covered with LPSQ-COOH (0.04 wt% solution in THF, $t_i = 15$ min, dried for 1 hour at ambient conditions) and immersed in pure THF for a given time. The samples were dried under ambient conditions for 24 hours and used for contact angle measurements.

Surface characterization. AFM images were recorded under ambient atmosphere using Nanoscope IIIa, MultiMode microscope (Veeco, Santa Barbara, CA) equipped with hot stage probe. The analysis (tapping mode) was carried out at room temperature (unless otherwise indicated). The probes were commercially available rectangular silicon cantilevers (RTESP from Veeco) with nominal radius of curvature in the 10 nm range, spring constant 20–80 N m⁻¹, and a resonance frequency lying in the 264–369 kHz. The images were recorded with the highest available sampling resolution, that is, 512 × 512 data points.

FTIR spectra were collected using a Nicolet 6700 spectrometer. The technique of attenuated total reflectance (ATR) was used for IR measurements, using germanium crystal attachment together with the mercury cadmium telluride detector (MCTD). The spectra were obtained by adding 64 scans at a resolution of 2 cm⁻¹.

Angle-resolved X-ray photoelectron spectra were recorded with a PHI 5000 VersaProbe™ – Scanning ESCA Microprobe™ (ULVAC-PHI, Japan/USA) equipped with a high resolution 180° spherical capacitor energy analyzer (sample-analyser Z axis tilt Θ of 15°, 25°, 35° and 45° with respect to the surface plane, samples were not pre-treated with argon sputter ion gun). The mica support in the analysed sample was covered with LPSQ-COOH by immersion in 0.06 wt% solution in THF ($t_i = 15$ min). The spectra were recorded using monochromatic Al-K α radiation ($h\nu = 1486.6$ eV) from an X-ray source operating at 100 μm spot size, 25 W, and 15 kV. The high-resolution XPS spectra

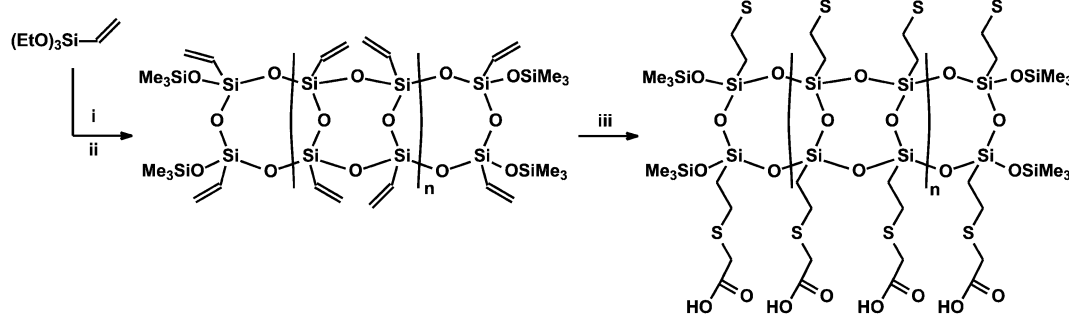
were collected with the analyzer pass energy of 23.5 eV and the energy step of 0.1 eV. The experimental data were processed using PHI MultiPak (Physical Electronics) software. The peaks were identified using NIST X-ray photoelectron spectroscopy database 20 (Version 4.1). A standard line shape analysis with a Gaussian fitting function was applied. The analysis was carried out at Mazovia Center for Surface Analysis (Institute of Physical Chemistry, Polish Academy of Sciences in Warsaw).

Contact-angle measurements. Static contact angles of sessile droplets of deionized water and glycerol (Chempur, pure p.a., anhydrous) at the film-air interface were measured at room temperature with a Rame-Hart NRL contact-angle goniometer equipped with a video camera JVC KYF 70B and drop-shape analysis software. The measurements were performed on untreated bare mica and on surfaces coated with LPSQ-COOH using dip-coating method as well as LPSQ-COOH and LPSQ-Vi cast with a slit applicator (film thickness of 60 μm). Static, advancing, and receding contact angles were measured right after the deposition of the liquid onto the film surface. The values of contact angles (standard deviation estimated) are an average of at least three measurements taken on different areas of the same sample. They are reported for a short contact time, strictly observed to diminish the effect of surface accommodation. Surface energies were estimated by the Owens-Wendt method using the values of advancing angles.

Results

1. Synthesis and properties of oligo[2-(carboxymethylthio)ethylsilsesquioxanes]

Linear oligosilsesquioxanes functionalized with side 2-(carboxymethylthio)ethyl groups and terminated with Me₃SiO units were prepared by photoinitiated thiol-ene addition of thioglycolic acid⁴² to their vinyl precursors (LPSQ-Vi) (Scheme 2). NMR spectroscopy confirmed that the addition proceeds regioselectively to give exclusively an anti-Markovnikov product: 2-(carboxymethylthio)ethyl moieties (all the pertinent synthetic and spectroscopic data can be found in the ESI†). Structure simulations



Scheme 2 Synthesis of LPSQ-COOH [i: potassium hydroxide, ii: acetic acid, hexamethyldilazane (HMDS), iii: thioglycolic acid, 2,2-dimethoxy-2-phenylacetophenone (DMPA), UV 365 nm].

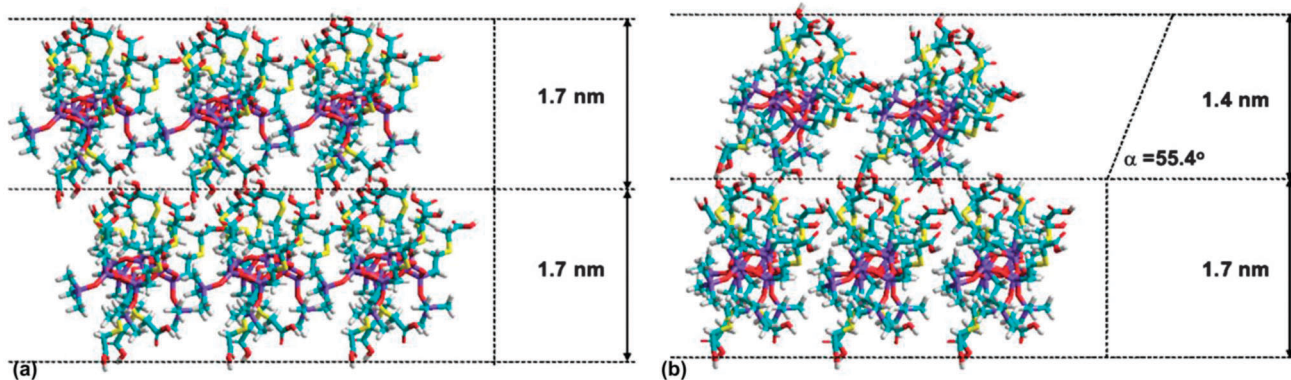


Fig. 1 Simulated structures of LPSQ-COOH oligomers self-assembled on mica: (a) vertical arrangement (b) tilted arrangement of the top layer (exemplary angle $\alpha = 55.4^\circ$).

(Fig. 1) confirmed that side 2-(carboxymethylthio)ethyl groups are placed perpendicularly to the double silsesquioxane chain that occupies the equatorial position. The product is soluble in some organic solvents (THF, dioxane) but insoluble in toluene and hexane.

Flexibility of the double-strand siloxane backbone in ladder silsesquioxanes, especially those bearing bulky side substituents,⁴³ is smaller than that of their linear single-chain analogs. DSC measurements carried out for LPSQ-COOH and LPSQ-Vi (Fig. ESI†-8) have shown that their devitrification occurs at temperatures higher than that typical for polysiloxanes.⁴⁴ However, the siloxane bonds in the studied materials retain to some extent their ease for reorientation. Glass transition temperatures found for LPSQ-COOH and LPSQ-Vi were almost the same, which suggests that both polymers have a similar degree of rotational freedom. It allows self-assembling species for the adjustment and formation of well-organized nanolayers at the solid/liquid interface. LPSQ-COOH undergoes several additional endothermic transitions that can be linked to a change of polymer chain packing at increased temperatures and rearrangement of inter- and intramolecular H-bonding between COOH groups in the polymer matrix. Such variability in strength is characteristic for hydrogen bonds and depends on their geometry.^{45,46}

2. Supramolecular assemblies of LPSQ-COOH on mica – AFM studies

The adsorption of polymers on solid surfaces from their solutions is governed by the conditions under which the polymer, surface and solvent interact. The formation of an ordered layered structure (including multilayer adsorption) at a liquid-solid interface is entropically disfavored and possible only if compensated by an energetic advantage of binding due to specific molecule-molecule and molecule-substrate interactions.^{47–49} Modeled processes of polymer absorption^{50–52} indicate that polymers can adopt a large number of configurations depending on the intrinsic flexibility of the polymer backbone and its affinity for the surface. The specific structure of LPSQ-COOH makes the polymer suitable for planar adsorption on reactive surfaces. Muscovite mica was chosen for the studies due to chemical specificity and its surface properties. Potassium ions

electrostatically bind the alternating mica sheets and neutralize the net negative charge associated with the presence of Brønsted acid sites [Si–O(H)-Al] within the basal (001) plane. Exfoliation of mica along the plane located in the K⁺ layer exposes large areas of molecularly smooth surface.³⁸ This makes mica an ideal AFM imaging substrate for biological systems^{24,25} and polymers at interfaces.^{53–55} Potassium ions can also form surface salts (e.g. carboxylates). Mica substrates were thus covered with thin layers of LPSQ-COOH by vertical immersion into a diluted solution or by the deposition of the dissolved material by spin-coating.

2.1. Analysis of polymer–substrate interactions and interlayer bonding. Adsorption of LPSQ-COOH onto mica and self-assembly into specifically arranged, layered structures was confirmed by the analysis of their respective AFM height profiles. The mechanism of adsorption of LPSQ-COOH on mica needs to be considered with respect to the molecular structure of the polymer and the possible intermolecular interactions. Structure simulations of LPSQ-COOH (Fig. 1) exhibit specific arrangement of side chains terminated with COOH groups with respect to the silsesquioxane backbone. While the above-mentioned thermodynamic principles are obeyed for rigid LPSQ-COOH, our studies showed that the configuration adjustment phase can be less decisive in the mechanism of adsorption. Topographic AFM images and height profile analysis suggest close packing within the strata, which is typical for high-affinity adsorption of macromolecules.⁵⁶ A maximum contact with the solid surface and compensation of repulsive forces between single adsorbed molecules is provided. It appears that macromolecules of LPSQ-COOH adsorb directly as they approach the surface and extend parallel to it with no loops and tails. The thickness of the nanolayers (average 1.6 nm for a single layer, Fig. 2) is in good agreement with the estimated molecule width (the distance between carboxylic groups placed at the opposite sides of silsesquioxane chain is constant). Similar to all other products of polycondensation, LPSQ-COOH exhibits a certain distribution of chain length and molecular weight. The oligomeric species are terminated with surface-inactive trimethylsilyl groups, which exclude the possibility of perpendicular orientation of macromolecules.

Macromolecules of LPSQ-COOH within a single monolayer are arranged horizontally with respect to the substrate surface

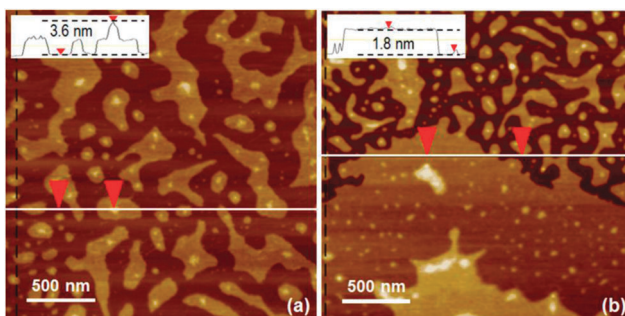


Fig. 2 AFM height image and the corresponding surface profiles of LPSQ-COOH dip coated on muscovite mica (0.045 wt% solution in THF, $t_i = 5$ s): (a) bilayer islands and (b) monolayer.

due to interactions between side groups and mica (Scheme 1). It can be assumed that, analogous to earlier reports concerning SAMs,^{27–30} LPSQ-COOH are adsorbed on mica through specific ionic interactions between K^+ ions and side COOH groups. Their importance in the adsorption process can be confirmed by ATR-FTIR and ARXPS (Sections 3 and 4), as well as by an exceptional difference in the behavior of LPSQ-COOH and LPSQ-Vi dip coated on mica from a solution in THF of the same concentration (Fig. ESI†-12 and ESI†-13). Hydrophobic material functionalized with vinyl groups forms droplets of 2.4 nm height ($t_i = 5$ s) that are scarcely distributed over the surface and grow in their height on the increase of t_i . LPSQ-COOH does not form ordered nanolayers on bare glass or hydrophobic surfaces (e.g. HF-treated silicon and APTES silanized glass) (Fig. ESI†-14). COOH groups situated at one side of the plane formed by double-strand silsesquioxane chains are involved in the interaction with mica. Other forced conformations are improbable, because otherwise the self-assembling system would be perturbed by the strata of different symmetry. Cyclic dimers, trimers, and linear catemeric structures (Scheme ESI†-1) are common binding arrangements for resonance-assisted hydrogen bonding in carboxylic groups, both on surfaces and in molecular crystals.^{57,58} They can guide the reorientation of molecules to optimize attractive/repulsive forces. Molecular modeling has shown that although the orientation of side 2-(carboxymethylthio)ethyl groups with reference to silsesquioxane chain is defined, they can slightly recline in relation to the axis perpendicular to the polymer backbone and become available for lateral molecule–molecule interactions (intra-molecular hydrogen bonding) within a single stratum. Hydroxyl oxygen atoms in such catemeric form are sterically accessible. These can act as acceptors of additional hydrogen bonds from other molecules of LPSQ-COOH, resulting in the formation of multi-layered structures (inter-layer hydrogen bonding).

2.2. Effect of coating parameters on the structure of the overlayer. The rate of adsorption of polymers is determined by the concentration and viscosity of their solutions. It was thus a question if macromolecules of LPSQ-COOH adsorb from solution separately or as aggregated clusters that can be more easily formed in concentrated solutions. Dynamic light scattering measurements (Fig. ESI†-15) did not detect defined agglomerates of LPSQ-COOH in solutions in THF of different concentration.

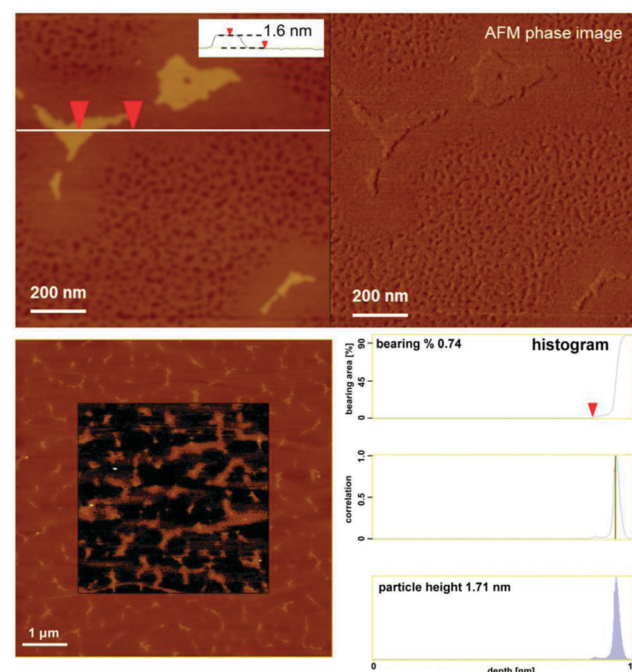


Fig. 3 Structure of LPSQ-COOH film dip coated on muscovite mica (0.0022 wt% in THF, $t_i = 5$ s, AFM height image and surface profile). Height histogram obtained from the AFM image shows the population of the top self-assembled layer (Sigma Scan analysis of a black/white version of the image indicate that brightest terraces (top layer) extent over ~3% of the analyzed surface).

The structure of adsorbed nanolayers (coverage, density, size and number of layers) was found to be very slightly concentration dependent. It was observed that even a short immersion in a very dilute solution (0.0022 wt%) results in complete monolayer coverage, decorated sparsely with subsequent (top) layers (Fig. 3). The multilayer model of adsorption that does not require the completion of the first layer before the formation of the next one seems to be obeyed. Various densities of surface coverage can be observed in different areas. The main part of the monolayer has a less compact structure, but patches surrounding the areas covered with the top layer are packed more tightly. These domains seem to grow from crystallization centers to the periphery, typically for films self-assembled from solutions. Self-assembling systems can accommodate by tilting chains on decrease of local packing density. Surface coverage and the density of packing increased with the polymer concentration and immersion time. It results in the formation of a well-organized surface (Fig. 4).

The nature of the adsorbate determines the packing density of monolayers and AFM data obtained for LPSQ-COOH–THF system show similar morphology of deposits for different coating conditions. Moreover, films of LPSQ-COOH that are obtained by spin coating solutions in THF (Fig. 5a) resemble closely those prepared by dip coating. The thickness of the main layer that covers most of the surface is 1.8 nm. It is partly covered with a top layer in the form of tilted islands of an average 1.3 nm height.

To estimate the effect of solvent on the structure of adsorbed material we have studied the morphology of LPSQ-COOH films

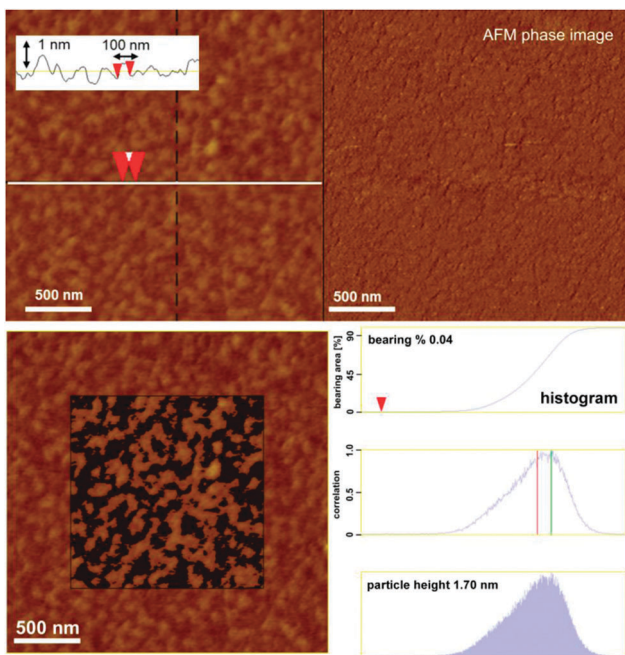


Fig. 4 High coverage of mica surface by LPSQ-COOH (0.051 wt% in THF, $t_i = 5$ min, dip coating, AFM height image and surface profile). The covering of analyzed surface (~80%) was estimated by Sigma Scan analysis of a black/white image.

spin coated onto mica from 0.06 wt% solution of LPSQ-COOH in a mixture of toluene and dioxane (1 : 2 v/v). The solvent ratio was selected to provide a good solubility of LPSQ-COOH using the lowest amount of polar solvent. It should be noted that LPSQ-COOH dissolves well in pure dioxane and toluene-dioxane mixtures (at the given ratio). The solutions are clear and transparent for at least 30 hours. However, DLS profiles of samples dissolved in dioxane or mixtures of dioxane-toluene are different than those in THF and THF-toluene (Fig. ESI†-16). The polymer tends to form discrete aggregates that finally sediment with time (>48 h).

The morphological comparison of micrographs indicates a considerable change in the structure of the film deposited from the freshly prepared solution in toluene-dioxane in a non-equilibrium spin coating process (Fig. 5b). Mica is covered completely with the base layer, but the top surface is not smooth. In this case, deposits formed misshapen spikes instead of lamellar structures. It is known that the type of monolayer growth can be stabilized by an appropriate solvent (solvent-induced polymorphism⁵⁷). Dip-coating experiments (Fig. 6) confirmed the importance of polymer substrate interactions and suggest that a lower rate of solvent evaporation could determine the structure obtained in the spin coating process. Samples prepared with 0.06 wt% solution in toluene/dioxane (1 : 2 v/v) are similar to those prepared using THF solutions. Micrographs also exhibited the effect of immersion time on the amount of adsorbed LPSQ-COOH. In conclusion, the studied material can aggregate in a poor solvent, but the specific surface interactions play a more important role in the assembly process.

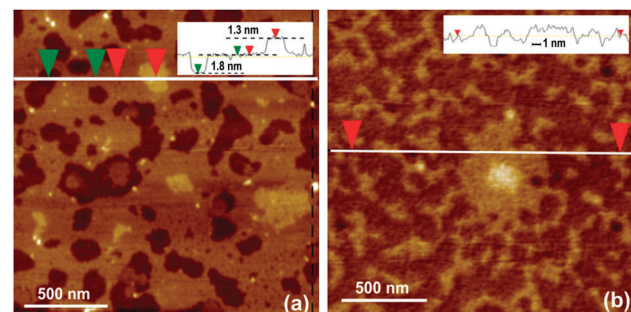


Fig. 5 Morphology of deposits of LPSQ-COOH (AFM topography and surface profile) spin coated onto mica plate using (a) 0.06 wt% solution in THF and (b) 0.06 wt% solution in toluene/dioxane (1 : 2 v/v).

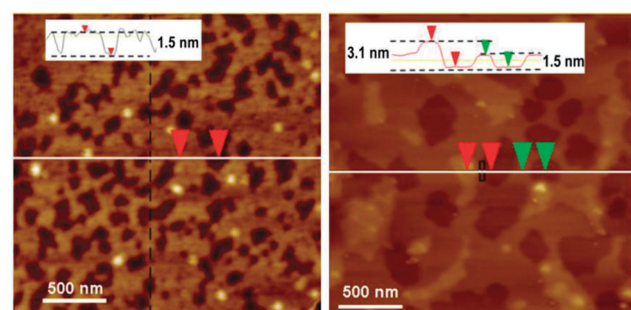


Fig. 6 Structure of self-assembled deposits of LPSQ-COOH dip-coated onto mica using 0.06 wt% solution in toluene/dioxane (1 : 2 v/v): (a) $t_i = 5$ s; (b) $t_i = 5$ min.

3. Analysis of polymer–substrate interactions by ATR-FTIR

Infrared spectrometry can be an excellent diagnostic tool for the identification of C=O groups, because their chemical behaviour is dependent on the structural environment.^{59–61} ATR-FTIR measurements were thus carried out to understand better the mechanism of adsorption of LPSQ-COOH on the surface of mica. Spectra were measured for the native LPSQ-COOH in bulk and after its adsorption on mica. The regions near 1700 cm^{-1} (C=O stretch), 1400 cm^{-1} (in plane O-H deformation), 1250 cm^{-1} (C-O stretch) and 920 cm^{-1} (out of plane O-H deformation) were used for the identification. Fig. 7 represents FTIR spectrum of the pure LPSQ-COOH in bulk. The assignments of the bands characteristic for pure LPSQ-COOH are given in Table ESI†-1. The C-S linkages and methyl rocking modes cannot be readily identified because their characteristic bands can be expected at wavelengths $<850\text{ cm}^{-1}$.⁵⁹ LPSQ-COOH dissolves only in polar solvents (strong solvent interaction effects can be expected), and it is impossible to obtain its non-hydrogen bonded spectra in dilute solutions.

Carboxylic acids exist normally in stable dimeric form with very strong hydrogen bridges between the carbonyl and hydroxyl groups of the two molecules. This association can persist even in the vapour state or in dilute solution in certain solvents. The shape of the C=O FTIR band (centered at 1710 cm^{-1}) in bulk LPSQ-COOH is clearly asymmetric with noticeable broadening at lower frequencies. Vibrations of carboxylic groups

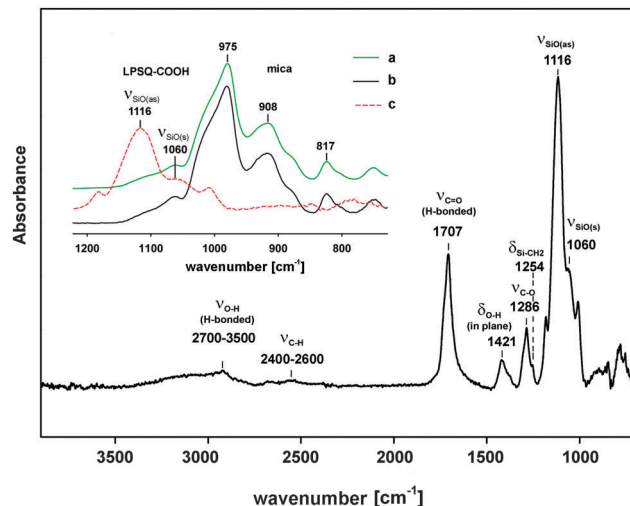


Fig. 7 ATR FT-IR spectra of native LPSQ-COOH (bulk) [the inset represents compared spectra of mica covered with LPSQ-COOH (a), freshly air-cleaved mica support (b) and native LPSQ-COOH (c)].

can be seen as two overlapping bands at 1721 and 1707 cm⁻¹. The shift of the C=O vibrational bands to lower wavenumbers is caused by hydrogen bonding. It can be thus surmised that carboxylic groups in bulk LPSQ-COOH are both in the form of hydrogen-bonded dimers as well as monomers. Alternatively, the 1721 cm⁻¹ peak may correspond to hydrogen-bonded -COOH of different geometry (looser forms of association). The formation of acyclic head-to-tail dimers with one strong hydrogen bridge and a secondary weak CH· · · O=C interaction was postulated as the initial step for the formation of their cyclic counterparts.^{62–64} The FTIR spectrum of the acyclic form shows O-H stretching frequencies intermediate between that of the monomer and the cyclic dimer. We were unable to distinguish between these two contributions at this point. However, as was earlier discussed, such interactions could be geometrically feasible in LPSQ-COOH.

FTIR spectrum of mica exhibits a strong Si-O apical vibration with a single mode evolution⁶⁵ and could not be subtracted as background. Consequently, the wavelength region >1200 cm⁻¹ could not be analyzed. However, some important specific interactions in the multilayer structure could be observed on the analysis of FTIR spectra (wavelength range 1850–1200 cm⁻¹) of samples prepared with solutions of LPSQ-COOH in THF of increasing concentration (Fig. 8). The spectrum of the first monolayer prepared with the least concentrated solutions [Fig. 8(b)] shows diffuse bands at 1750–1600 cm⁻¹ and 1500–1350 cm⁻¹ and a small peak at about 1260 cm⁻¹. The position of the latter band did not change with increasing thickness of the adsorbed layer. It corresponds to Si-CH₃ band in bulk LPSQ-COOH (Table ESI†-1) and confirms the adsorption of the polymer on mica.

Ionization of a carboxylic acid moiety (formation of COO- group) results in the equilibration of two oxygen atoms attached to the same carbon atom (resonance between the two C=O bonds) with the disappearance of C=O absorption. Two broad bands near 1550 cm⁻¹ (anti-symmetrical) and 1400–1300 cm⁻¹ (symmetrical vibration)^{59,60,66} should appear in the spectrum

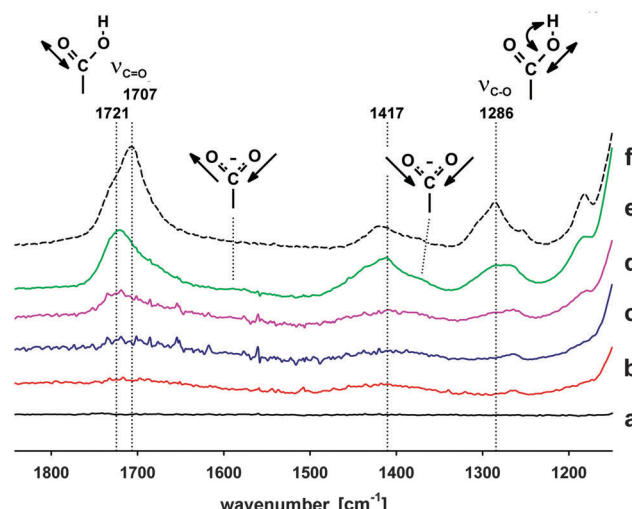


Fig. 8 ATR-FTIR spectra [(a–e) normalized to $\nu(\text{Si}-\text{O})$ 975 cm⁻¹] of the characteristic regions for C=O and C–O stretching and the –OH bending regions at 1750–1200 cm⁻¹ for native LPSQ-COOH (f) and after its coating on mica using a dip coating technique [(a) clean mica support, coated using: (b) 0.002 wt% (as in Fig. 3), (c) 0.022 wt%, (d) 0.045 wt%, and (e) 0.051 wt% solution in THF]. The spectrum of freshly cleaved mica was used as a reference.

on the formation of carboxylate groups, as in the proposed model of adsorption. Indeed, they can be observed, particularly on the formation of monolayers from diluted solution (Fig. 8, traces b–d). It suggests that LPSQ-COOH can be chemisorbed as a carboxylate onto the mica surface. The type of interaction between the carboxylate moiety and the metal atom can be diagnosed by FTIR.^{67–69} Unfortunately, the intensity of peaks in the recorded spectra is too low to conclude whether carboxylate groups of LPSQ-COOH are coordinated symmetrically to the K atoms.

The C=O stretch band of dimeric species (1707 cm⁻¹) is substantially diminished in the spectrum of the coated samples. However, the C=O band at 1721 cm⁻¹ becomes more defined on the increase of the silsesquioxane layer thickness. This can be explained by the relative increase of the amount of -COOH groups arranged in hydrogen-bonded layers *versus* carboxylates involved in ionic interactions with surface. This finding is in agreement with the proposed model of adsorption.

4. Structure of LPSQ-COOH films analyzed by ARXPS

Photoelectron spectroscopy analysis was used to characterize LPSQ-COOH and the layers adsorbed on mica surfaces (Fig. 9). The XPS spectrum of mica was used as a reference. The elements emitting photoelectrons in LPSQ-COOH are specified as silicon [Fig. ESI†-17, Si2p core-level at 101.0 eV with Si2p_{3/2} (100.8 eV) and Si2p_{1/2} (101.4 eV) components], carbon [Fig. 10, C1s envelope that can be resolved into four contributions referred to neutral sp³ carbon (C-C) at 283.3 eV and three peaks with modified electron environment positioned at 284.2 eV (C-S), 285.2 eV (C-O) and 288.1 eV (C=O)], oxygen (Fig. ESI†-18 O1s, 530.9 eV, with C=O bonding at 531.9 eV, H-O-C bonding at 532.8 eV) and sulphur [Fig. 11, S2p, with closely spaced spin-orbit components S2p_{3/2} (162.2 eV) and S2p_{1/2} (163.5 eV)].

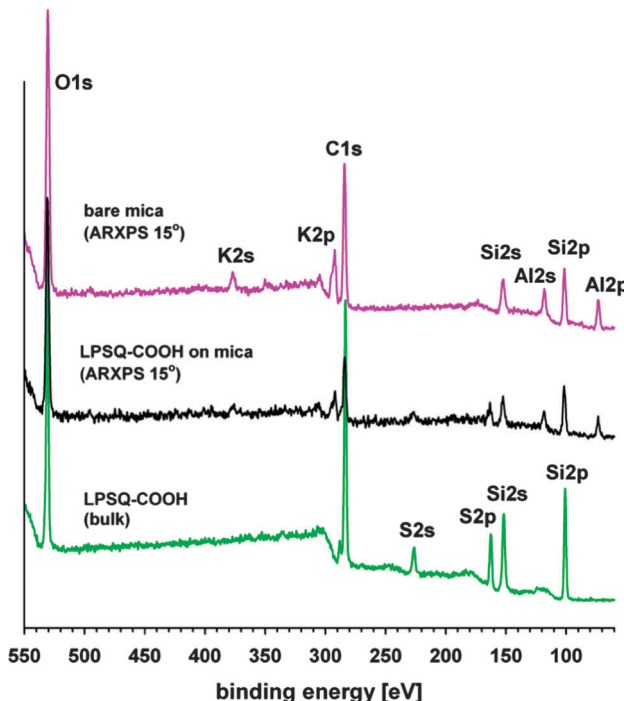


Fig. 9 XPS spectra of LPSQ-COOH before and after adsorption on mica compared to a reference XPS spectrum of air-cleaved mica.

The XPS spectrum of air-cleaved mica surfaces includes peaks corresponding to silicon (Si2p 101.2 eV), oxygen (O1s 530.4 eV), potassium (K2p, 292.4 eV) and aluminium (Al2p, 73.6 eV). A broad C1s peak at 285.2 eV in mica's grazing emission XPS spectrum indicates the presence of adventitious carbon species.⁷⁰ Apparent shifts in binding energy (comparing to C1s of LPSQ-COOH) are due to the existence of strong dipole fields at the surface.⁷¹

The expected (C1s, O1s, Si2p, S2p) core level peaks were detected in the ARXPS spectra of adsorbed LPSQ-COOH. Due to surface adsorption effects, the resolution of XPS spectra is poor and it is difficult to differentiate Si and O atoms contained in the silsesquioxane overlayer from those belonging to the adsorbent. All peaks are slightly shifted to higher energies. It is postulated that LPSQ-COOH attachment to mica is due to the formation of a surface salt – potassium carboxylate. As shown by the analysis of model compounds,⁷² the two oxygen atoms in the carboxylate group $[-\text{C}(\text{O})\text{O}-\text{K}^+]$ would have the same physical and chemical properties due to the effect of charge delocalization; thus, they should have the same binding energy (about 532.4 eV).

However, only 3 peaks were observed in the C1s spectrum of LPSQ-COOH adsorbed on mica. A general broadening of the C1s core level envelope and the fitted peaks is observed. Distinctively, the primary C=O peak (288.1 eV) disappeared, which could be due to the formation of carboxylate ($-\text{COO}-$) moieties (shifting the characteristic peak, widened by the effect of surface adsorption, to slightly higher binding energies⁶⁹). The C1s envelope is similar in XPS spectra recorded at different take-off angles, which points to the surface adsorption effect as an origin of peak widening. The O1s peak asymmetry observed

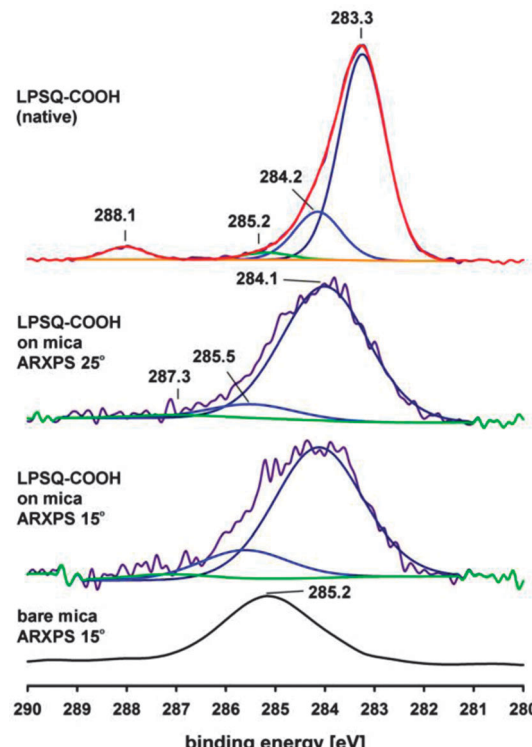


Fig. 10 XPS C1s peak deconvolution in the studied samples (native and adsorbed LPSQ-COOH compared to bare, air-cleaved mica).

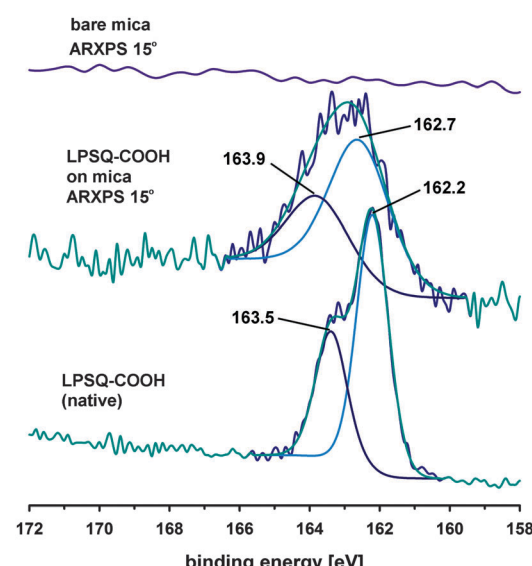


Fig. 11 XPS Sp2 peak deconvolution and binding energy differences observed for bulk and adsorbed LPSQ-COOH.

for native LPSQ-COOH is not retained and photoelectron peaks corresponding to C=O and H–O–C groups cannot be distinguished in the adsorbed samples.

The surface effect is quite pronounced and it can be observed also for atoms not involved directly in interactions with the mica surface. The closely spaced spin-orbit components S2p_{3/2} (162.2 eV) and S2p_{1/2} (163.5 eV) of the peak corresponding to sulphur atoms

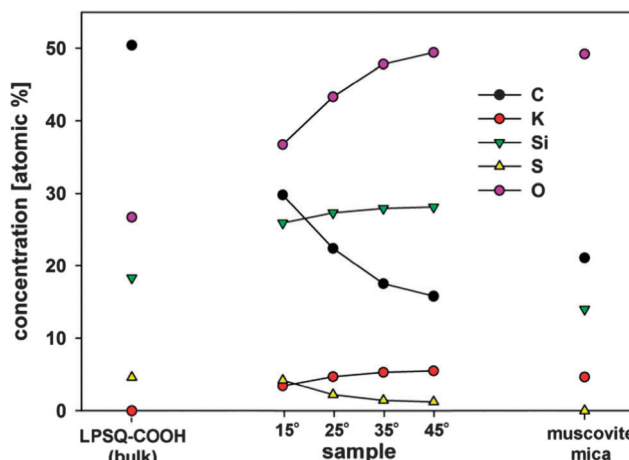


Fig. 12 XPS element concentration plots in native LPSQ-COOH (take-off angle Θ 45°), air-cleaved muscovite mica (take-off angle Θ 15°) and a sample of mica coated with self-assembled layers of LPSQ-COOH (at increasing Θ and beam sampling depth).

are narrow in the spectrum of native LPSQ-COOH. Their width increases significantly in the spectrum of adsorbed oligosilsesquioxane (Fig. 11).

In addition to the basic structural parameters, XPS results related to other features of the coating layers were analysed. ARXPS spectra taken for several photoelectron take-off angles are sensitive to changes in atomic concentration within the sample depth. The ratios of normalized intensities of the characteristic photoelectrons obtained with ARXPS are presented on Fig. 12 for the native LPSQ-COOH, mica substrate and the LPSQ-COOH overlayer adsorbed on mica (plotted *versus* the take-off angle function Θ). The atomic concentrations of adsorbed LPSQ-COOH presented in Fig. 12, differ from those of the bulk sample and vary with Θ . Potassium and sulphur can be found uniquely in the substrate or in the overlayer and can be used as indicators of the finite thickness of the coating layer. The concentration of carbon decreases with increasing of the effective sampling depth (to the value smaller than that observed for air-cleaved mica, which supports adventitious origin of the latter). As expected, the molar fraction of the elements shared in the coating and the substrate (Si, O) tends to rise with the increase of the take-off angle.

5. Thermal and solvolytical stability of LPSQ-COOH-mica system

Macroscopic control of surface properties requires stability at a molecular level. The rearrangement of surface structures can occur under specific conditions (*e.g.* upon exposure to a good solvent or surface diffusion phenomena at heating) due to increasing degrees of freedom, if the entropic penalty of chain extension is more significant than the polymer-surface interactions. The layered structure of spin-coated samples of LPSQ-COOH on mica is retained under ambient conditions (Fig. ESI†-19). Further studies suggested that nanolayers of LPSQ-COOH adsorbed and self-assembled on mica *via* hydrogen bonding are also thermally stable in air.

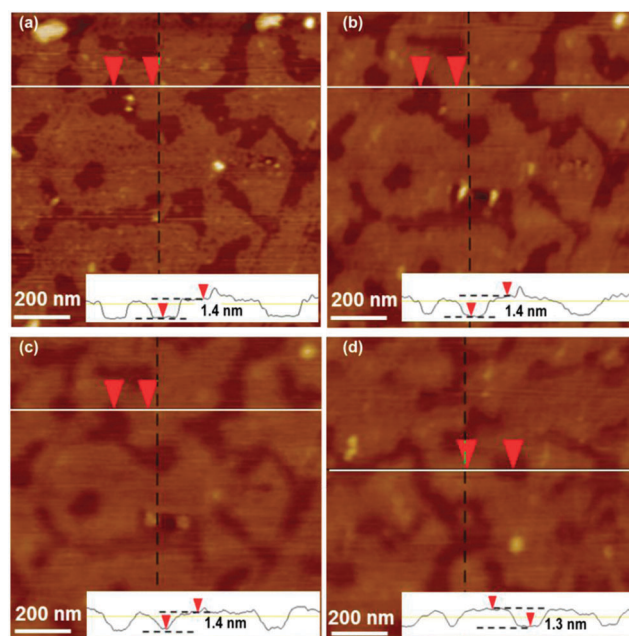


Fig. 13 AFM height images and surface profiles of LPSQ-COOH (0.02% in THF, $t_i = 5$ s) dip coated onto mica, recorded at (a) 24 °C (equilibrium structure), (b) 38 °C, (c) 60 °C and (d) after cooling to 30 °C.

Thickness and shape of the top layers were analyzed using hot-stage AFM. The temperatures were chosen with respect to thermal transitions characteristic for the studied polymer (Fig. ESI†-8). Mica plates covered with LPSQ-COOH were first scanned at room temperature (Fig. 13a). The sample was then heated (at rate 5 °C per min) to 38 °C (Fig. 13b) and then to 60 °C (Fig. 13c). The sample surface was scanned with an AFM probe after a short incubation time (3 minutes). Roughness profiles showed that the surface structure remained smooth within the studied temperature range. Nanolayers are defined and firmly bound to the surface of mica and the underlying polymeric material. On increasing the temperature above that defined by the second endothermic peak, one can observe a slight softening of the top layer. Despite the increased softness, the topographic pattern on the surface remains unchanged. The sample was then cooled to 30 °C. The cooling was inertial and it took ~15 minutes to change the temperature of the sample. The studied topographic motif endures and lamellar organization of the material is evident.

Another important aspect of interfacial self-assembly is thermodynamic control of adsorbed systems and equilibrium between the molecules adsorbed at the surface and those dissolved in the supernatant liquid phase. Transport phenomena and degrafting of polymers from the surface can impact the process. However, experimental results suggest that the stability of layered structures of LPSQ-COOH is reinforced by chemisorption and self-assembly on mica. Mica tiles, already coated with LPSQ-COOH (dip-coating, 0.04 wt% in THF, $t_i = 15$ min), were immersed in pure THF or pure toluene for 15 minutes. AFM studies showed good surface coverage after the washing test. Wettability studies (part 6) suggest that the lamellar

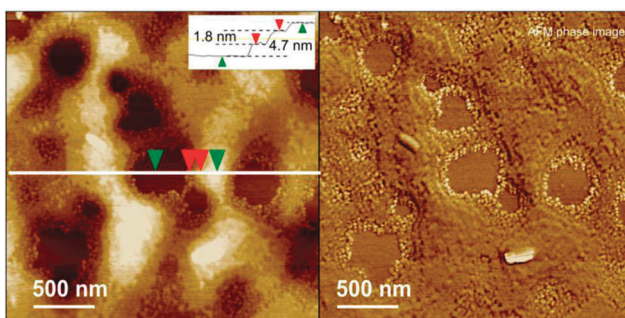


Fig. 14 AFM height image and surface profile of LPSQ-COOH on muscovite mica (0.045 wt% in THF, 27 °C, $t_i = 10$ h, dip coating).

arrangement in thin layers is durable and resists solvolysis by THF for at least 15 minutes.

An experiment was carried out to analyze stability of the adsorbed layer on prolonged immersion time. A sample of mica was placed for 10 h in a solution of LPSQ-COOH (0.045 wt% in THF) and placed in a tightly closed container. An AFM image shows that the adsorbed polymer is arranged in smooth, layered structures and regions overspread with granular patterns made of the same material (Fig. 14). It can be explained by a limited range of surface controlled adsorption. In such a case, macromolecules tend to adsorb in a disordered manner in the outermost layers (the effect can be augmented by decreasing the concentration of the solution). It can be also expected that the detachment associated with solvolysis of the least-bonded macromolecules after long immersion times is easier at certain thickness levels.

6. Wettability of LPSQ-COOH coated on mica

Wettability of the studied surfaces (bare mica, samples of LPSQ-COOH dip-coated or cast onto mica, and LPSQ-Vi cast onto mica) was determined by contact-angle measurements (sessile drop technique) using water and glycerol as reference liquids. Static, advancing and receding contact angles were measured and the surface free energy (polar and dispersive components) was calculated. It was found that all LPSQ-COOH samples are hydrophilic. Part of the polar component in their surface energy is considerably larger than the dispersive one (Fig. 15). A significant difference in wettability has been reproducibly observed depending on the method of coating. The surface energy of a film of LPSQ-COOH cast on mica with a slit applicator (film thickness ~60 μm) is smaller than that of the dip-coated sample (0.04 wt% solution in THF, $t_i = 15$ minutes). This can be explained by the different arrangement of molecules of LPSQ-COOH in the coating. Polar carboxylic groups situated at the top side of adsorbed nanolayers are forced to adopt an unfavorable orientation with respect to hydrophobic air, but it makes the surface exceptionally hydrophilic. COOH groups in macromolecules that are not arranged in a lamellar way (slit-coated layer) are less accessible for the formation of hydrogen bonds with reference liquids during the measurement. It was also found that the surface energy of hydrophobic LPSQ-Vi is similar to that of slit-cast LPSQ-COOH, except that its major component is formed by dispersive forces. The difference between the

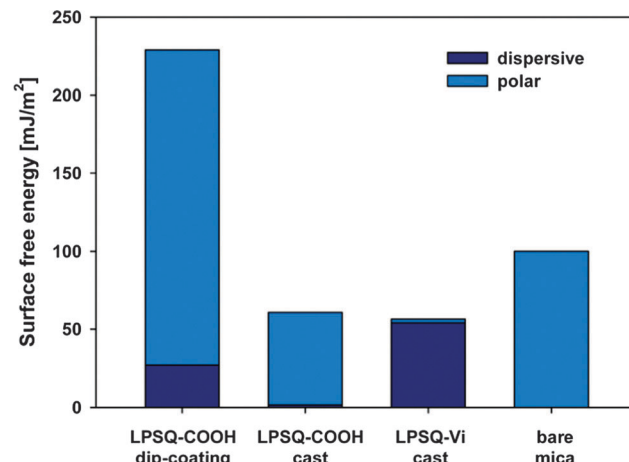


Fig. 15 Surface energy of studied coatings determined by wetting angle measurements.

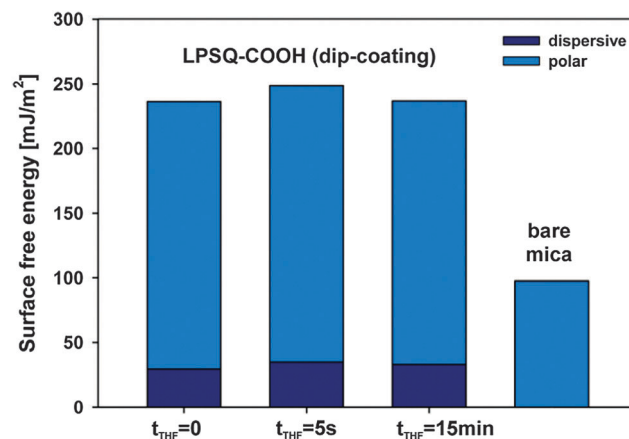


Fig. 16 Solvolytic stability of LPSQ-COOH adsorbed on mica (samples immersed in THF).

receding and advancing angle is smaller than that recorded for LPSQ-COOH. The energy of hydrophilic mica is comparable to the reported data.⁷³

Lamellar organization of LPSQ-COOH and firm interactions with mica are important for the surface solvolytic stability profile. Dip-coated samples (0.04 wt% solution in THF, $t_i = 15$ minutes) were immersed in pure THF and toluene for a given time (5 s and 15 minutes) at room temperature. Contact-angle measurements show that the surface properties did not change (Fig. 16).

Conclusions

In this study, we have combined different experimental and computational techniques, including atomic force microscopy, XPS and ATR-FTIR spectroscopy, as well as molecular structure simulations to analyse the process of the self-assembly of ladder oligosilsesquioxanes bearing side carboxylic groups (LPSQ-COOH) on mica. AFM studies have shown that linear macromolecules of LPSQ-COOH can adsorb horizontally on the surface of

muscovite mica and self-assemble into layered structures. Alternative adsorption mechanisms and orientation with brush-like conformations of the silsesquioxane chains is excluded. The ATR-FTIR spectra confirmed interactions between –COOH groups of LPSQ-COOH and the surface of mica. The XPS spectra demonstrated the variation of C1s and O1s binding in C=O groups before and after adsorption.

Organization of LPSQ-COOH within the adsorbed overlayer results from both molecule-to-substrate and molecule-to-molecule bonding. The molecular interactions are determined by the specific position of functional groups with respect to the rigid double-chain silsesquioxane backbone. Individual layers of LPSQ-COOH are stacked due to the formation of hydrogen bonds between carboxylic groups at interfaces.

Surface energy measurements confirmed the horizontal arrangement of LPSQ chains suggested by AFM, with COOH groups in the interlayers and pointing away from the surface. This specific arrangement of COOH groups makes the surface highly hydrophilic and solvolytically stable. The self-assembled structures anchored to the surface do not undergo rearrangements due to surface diffusion, even at increased temperatures. The particular properties and stability of this LPSQ-COOH-mica system are promising for the preparation of patterned surfaces with immobilized COOH groups as specific ligands for cell-culture studies. LPSQ-COOH can be used not only for surface coating but also as an ink for the micropatterning of mica (these results are currently in preparation for publication).

Acknowledgements

The authors thank Polish National Science Centre for the financial support within grant DEC-2011/03/B/ST5/02672 “Studies on preparation and structurization of new hybrid materials”. We also thank Dr J. W. Sobczak and Dr K. Nikiforow Mazovia Center for Surface Analysis (Institute of Physical Chemistry, Polish Academy of Sciences in Warsaw) for ARXPS data.

Notes and references

- 1 G. A. Somorjai and Y. Li, *Proc. Natl. Acad. Sci. U. S. A.*, 2011, **108**, 917.
- 2 G. A. Hudalla and W. L. Murphy, *Soft Matter*, 2011, **7**, 9561.
- 3 Y. Arima and H. Iwata, *Biomaterials*, 2007, **28**, 3074.
- 4 M. L. B. Palacio and B. Bhushan, *Philos. Trans. R. Soc., A*, 2012, **370**, 2321.
- 5 M. Franco and P. F. Nealey, *J. Biomed. Mater. Res., Part A*, 2000, **52**(2), 261.
- 6 B. G. Keselowsky, D. M. Collard and A. J. García, *Proc. Natl. Acad. Sci. U. S. A.*, 2005, **102**, 5953.
- 7 K. B. McClary, T. Ugarova and D. W. Grainger, *J. Biomed. Res.*, 2000, **50**, 428.
- 8 N. Faucheu, R. Schweiss, C. Werner and T. Groth, *Biomaterials*, 2004, **25**, 2721.
- 9 M. A. Lan, C. A. Gersbach, K. E. Michael, B. G. Keselowsky and A. J. García, *Biomaterials*, 2005, **26**, 4523.
- 10 M. H. Lee, P. Ducheyne, L. Lynch, D. Boettiger and R. J. Composto, *Biomaterials*, 2006, **27**, 1907.
- 11 B. Tarasevich, C. Tidwell, S. I. Ertel and S. Atre, *Langmuir*, 1997, **13**, 3404.
- 12 J. M. Curran, R. Chen and J. A. Hurt, *Biomaterials*, 2005, **26**, 7057.
- 13 J. M. Curran, R. Chen and J. A. Hunt, *Biomaterials*, 2006, **27**, 4783.
- 14 P. M. Mendes, *Chem. Soc. Rev.*, 2008, **37**, 2512.
- 15 X. Liu and S. Wang, *Chem. Soc. Rev.*, 2014, **43**, 2385.
- 16 A. Ulman, *Chem. Rev.*, 1996, **96**, 1533.
- 17 W. A. Marmisollé, D. A. Capdevila, E. de la Llave, F. J. Williams and D. H. Murgida, *Langmuir*, 2009, **29**, 5351.
- 18 J.-W. Park, H. Kim and M. Han, *Chem. Soc. Rev.*, 2010, **39**, 2935.
- 19 D. Li, Q. Zheng, Y. Wang and H. Chen, *Polym. Chem.*, 2014, **5**, 14.
- 20 W. Senaratne, L. Andruzzi and Ch. K. Ober, *Biomacromolecules*, 2005, **6**, 2427.
- 21 M. E. Welch and Ch. K. Ober, *J. Polym. Sci., Part B: Polym. Phys.*, 2013, **51**, 1457.
- 22 J. A. Dhotel, Z. Chen, L. Delbreilh, B. Youssef, J.-M. Saiter and L. Tan, *Int. J. Mol. Sci.*, 2013, **14**, 2303.
- 23 E. Busseron, Y. Ruff, E. Moulin and N. Giuseppone, *Nanoscale*, 2013, **5**, 7098.
- 24 W. W. Leow and W. Hwang, *Langmuir*, 2011, **27**, 10907.
- 25 R. W. Loo and M. C. Goh, *Langmuir*, 2008, **24**, 13276.
- 26 M. Sun, A. Stetco and E. F. Merschrod, *Langmuir*, 2008, **24**, 5418.
- 27 J. A. Heredia-Guerrero, M. A. San-Miguel, M. S. P. Sansom, A. Heredia and J. J. Benítez, *Z. Phys. Chem.*, 2010, **12**, 10423.
- 28 J. A. Heredia-Guerrero, M. A. San-Miguel, M. S. P. Sansom, A. Heredia and J. J. Benítez, *Langmuir*, 2009, **25**, 6869.
- 29 J. J. Benítez, J. A. Heredia-Guerrero, F. M. Serrano and A. Heredia, *J. Phys. Chem. C*, 2008, **112**, 16968.
- 30 J. J. Benítez, J. A. Heredia-Guerrero and A. Heredia, *J. Phys. Chem. C*, 2007, **111**, 9465.
- 31 J. Chen, A. R. Murphy, J. Esteve, D. F. Ogletree, M. Salmeron and J. M. J. Fréchet, *Langmuir*, 2004, **20**, 7703.
- 32 Y. L. Lyubchenko, L. S. Shlyakhtenko and T. Ando, *Methods*, 2011, **54**, 274.
- 33 Z. Liu, Z. Li, H. Zhou, G. Wei, Y. Song and L. Wang, *Microsc. Res. Tech.*, 2005, **66**, 179.
- 34 N. Crampton, W. A. Bonass, J. Kirkham and N. H. Thomson, *Langmuir*, 2005, **21**, 7884.
- 35 L. S. Shlyakhtenko, A. A. Gall, J. J. Weimer, D. D. Hawn and Y. L. Lyubchenko, *Biophys. J.*, 1999, **77**, 568.
- 36 H. Okusa, K. Kurihara and T. Kunitake, *Langmuir*, 1994, **10**, 3577.
- 37 S. Kim, S. H. K. Christenson and J. E. Curry, *Langmuir*, 2002, **18**, 2125.
- 38 B. Liberelle, X. Banquy and S. Giasson, *Langmuir*, 2008, **24**, 3280.
- 39 J. Wood and R. Sharma, *Langmuir*, 1994, **10**, 2307.
- 40 Z.-H. Liu, N. M. D Brown and A. McKinley, *Appl. Surf. Sci.*, 1997, **108**, 319.

- 41 A. Kowalewska and M. Nowacka, *Silicon*, 2015, **7**, 133.
- 42 W.-B. Zhang, Y. Li, X. Li, X. Dong, X. Yu, Ch.-L. Wang, C. Wesdemiotis, R. P. Quirk and S. Z. D. Cheng, *Macromolecules*, 2011, **44**, 2589.
- 43 A. Kowalewska, W. Fortuniak and B. Handke, *J. Organomet. Chem.*, 2009, **694**, 1345.
- 44 P. R. Dvornic, Silicon-Containing Polymers, in *The Science and Technology of Their Synthesis and Applications*, ed. R. G. Jones, W. Ando and J. Chojnowski, Springer Science + Business Media B.V., Dordrecht, 2000, ch. 7, pp. 185–212.
- 45 S. J. Grabowski, *J. Phys. Chem. A*, 2001, **105**, 10739.
- 46 M. Ziolkowski, S. J. Grabowski and J. Leszczyński, *J. Phys. Chem. A*, 2006, **110**, 6514.
- 47 G. J. Fleer and J. Lyklema, in *Adsorption from Solution at the Solid/Liquid Interface*, ed. G. D. Parfitt and C. H. Rochester, Academic Press, New York, 1983, pp. 153–220.
- 48 G. M. Whitesides, J. P. Mathias and C. T. Seto, *Science*, 1991, **254**, 1312.
- 49 L. Liu and Q.-X. Guo, *Chem. Rev.*, 2001, **101**, 673.
- 50 N. Källrot, M. Dahlqvist and P. Linse, *Macromolecules*, 2009, **42**, 3641.
- 51 C. Bellmann, in *Polymer Surfaces and Interfaces*, ed. M. Stamm, Springer-Verlag, Berlin/Heidelberg, 2008, ch. 12, pp. 235–240.
- 52 P. Linse and N. Källrot, *Macromolecules*, 2010, **43**, 2054.
- 53 O. J. Rojas, Encyclopedia of Surface and Colloid Science, in *Adsorption of polyelectrolytes on mica*, ed. A. Hubbard, Marcel Dekker Inc., New York, 2002, pp. 517–535.
- 54 F. Zhao, Y.-K. Du, P. Yang, J. Tang and X.-C. Li, *Colloid Polym. Sci.*, 2005, **283**, 1361.
- 55 R. Koestner, Y. Roiter, I. Kozhinova and S. Minko, *Langmuir*, 2011, **27**, 10157.
- 56 M. Kosmulski, *Chemical Properties of Material Surfaces*, Marcel Dekker Inc., New York/Basel, 2001, ch. 4, pp. 503–505.
- 57 M. Lackinger and W. M. Heckl, *Langmuir*, 2009, **25**, 11307.
- 58 P. Gilli, V. Bertolasi, V. Ferretti and G. Gilli, *J. Am. Chem. Soc.*, 1994, **116**, 909.
- 59 I. J. Belamy, *The Infra-red Spectra of Complex Molecules*, Chapman and Hall Ltd., London, 3rd edn, 1975, pp. 183–202, 374–389, 397–398.
- 60 B. Smith, *Infrared Spectral Interpretation – A Systematic Approach*, CRC Press LLC, 1999, p. 103.
- 61 J. Coates, Encyclopedia of Analytical Chemistry, in *Interpretation of Infrared Spectra, A Practical Approach*, ed. R. A. Meyers, John Wiley & Sons Ltd, Chichester, 2000, pp. 10815–10837.
- 62 S. T. Shipman, P. C. Douglass, H. S. Yoo, C. E. Hinkle, E. L. Mierzejewskia and B. H. Pate, *Phys. Chem. Chem. Phys.*, 2007, **9**, 4572.
- 63 F. Madeja, M. Havenith, K. Nauta, R. E. Miller, J. Chocholoušová and P. Hobza, *J. Chem. Phys.*, 2004, **120**, 10554.
- 64 W. Sander and M. Gantenberg, *Spectrochim. Acta, Part A*, 2005, **62**, 902.
- 65 B. Velde, *Am. Mineral.*, 1978, **63**, 343.
- 66 V. Doan, R. Köpppe and P. H. Kasai, *J. Am. Chem. Soc.*, 1997, **119**, 9810.
- 67 F. P. Rotzinger, J. M. Kesselman-Truttmann, S. J. Hug, V. Shklover and M. Grätzel, *J. Phys. Chem. B*, 2004, **108**, 5004.
- 68 Z. Lu, A. Karakoti, L. Velarde, W. Wang, P. Yang, S. Thevuthasan and H.-F. Wang, *J. Phys. Chem. C*, 2013, **117**, 24329.
- 69 N. Wu, L. Fu, M. Su, M. Aslam, K. C. Wong and V. P. Dravid, *Nano Lett.*, 2004, **4**, 383.
- 70 H. Poppe and A. G. Elliot, *Surf. Sci.*, 1971, **24**, 149.
- 71 K. G. Bhattacharyya, *J. Electron Spectrosc. Relat. Phenom.*, 1993, **63**, 289.
- 72 B. Lindberg, A. Berndtsson, R. Nilsson, R. Nyholm and O. Exner, *Acta Chem. Scand., Ser. A*, 1978, **32**, 353.
- 73 H. K. Christenson, *J. Phys. Chem.*, 1993, **97**, 12034.